Electronic Journal of Differential Equations, Vol. 2022 (2022), No. 28, pp. 1–22.
ISSN: 1072-6691. URL: http://ejde.math.txstate.edu or http://ejde.math.unt.edu

MATHEMATICAL MODELS FOR THE TRANSMISSION OF MALARIA WITH SEASONALITY AND IVERMECTIN

ZHIHONG ZHAO, SHAOCHUN LI, YULAN LU

Abstract. Ivermectin has shown good effects for malaria control in clinical trial stages because it can kill mosquitoes feeding on recently treated individuals. In this article, we formulate and analyze a novel delay malaria transmission model taking into account seasonality and ivermectin. We show that the dynamics of the model is totally determined by the basic reproduction ratio R_0; that is, malaria will gradually die out if $R_0 < 1$ and will persist if $R_0 > 1$. Numerically, we verify the obtained theoretical results and evaluate the effect of ivermectin by related data of Kenya. We find that our simulation of the impact agrees with the prediction of the existing clinical trials in which it takes at least 25 years to eliminate malaria from Kenya with malaria control measures intact.

1. Introduction

Malaria is an acute febrile disease caused by *Plasmodium* microorganisms spread to humans by infected adult female *Anopheles* mosquitoes. The disease accounts for 241 million infectious in 87 malaria endemic countries and 627,000 deaths worldwide, with about 80% of malaria deaths occurring in children under 5 years of age in 2020 [33]. Moreover, 95% and 96% of malaria cases and deaths occur in Africa.

Mosquitoes as a major vector of malaria transmission have long been of interest to entomologists. Since the life cycle of mosquitoes is strongly correlated with season, then the trend toward malaria is most likely to follow the climate pattern [1, 10]. For instance, warmer temperature, which increases mosquito activity and lifespan, lead to mosquito bites more frequently. In addition, the temperature sensitivity of malaria parasites to mosquito hosts has long been established [15, 19].

After a long period of anti-malarial interventions, we found that *Plasmodium* falciparum infection prevalence in endemic Africa halved and the incidence of clinical disease fell by 40% between 2000 and 2015. Indoor residual spraying and insecticide-treated nets, the most widespread intervention, were by far the largest contributor (68% of cases averted) from 2000 to 2015 [4]. But still below target levels, there is an urgent need for additional tools to treat and control malaria, with the development of *Plasmodium* resistance to insecticides and drugs [20].

Ivermectin is a blocking drug that targets the vector itself, it works primarily by binding to glutamate-gated chlorine channels in nerve and muscle, leading to

2020 *Mathematics Subject Classification.* 92B05, 37N25.
Key words and phrases. Malaria model; ivermectin; time delay; basic reproduction ratio; sensitivity analysis.

Submitted November 16, 2021. Published April 7, 2022.

hyperpolarization, paralysis and death of the invertebrate, including mosquitoes, and might inhibiting sporozoite development [6, 7]. It is the only avermectin class of endectocides that is available for human use from 1987 [6], and more than 416.8 million treatments have been distributed for mass drug administrations (MDA) to eliminate onchocerciasis and lymphatic filariasis in 2020 [16]. Higher doses is well tolerated in human beings up to 2000 $\mu g/kg$. It can be seen that ivermectin has an excellent safety profile [25]. Several experiments have shown that the mosquitocidal effect of 150-200 $\mu g/kg$ single doses of ivermectin are short-lived around 5-6 days [7]. Three doses of 300 $\mu g/kg$ given over 3 days has a mosquitocidal effect in humans for 28 days against *Anopheles gambiae* sensu stricto [25]. It can be seen through those studies that ivermectin can reduce lifespan of mosquitoes, that means they are less likely to live long enough to complete sporogony and become infectious. Furthermore, unlike traditional vector control tools (e.g. indoor residual spraying and long-lasting insecticidal nets), ivermectin can reduce the likelihood of cross-resistance with existing insecticides [24, 25]. These results indicate that ivermectin has many attractive qualities as a novel malaria control tool, it targets mosquitoes regardless of feeding location or time. As mentioned above, we intend to formulate a mathematical model to investigate the impact of ivermectin on malaria transmission.

The earliest malaria transmission model was the Ross-McDonald model [21]. On this basis, extensive research have been developed to study malaria transmission dynamics including different factors, such as seasonality, time- delay, impact of various control strategies, spatial effects, stage structure of mosquitoes and humans and so on, see e.g. [2, 5, 9, 22, 30, 32] and references therein. Recently, [18] modelled the effect of ivermectin on malaria transmission control by ordinary differential equations and the results showed that ivermectin was significantly more effective in malaria control compared to the no-intervention state. In this paper, we formulate a novel delay malaria transmission model taking into account seasonality and ivermectin, use the theoretical approach to analyze our model's dynamical behavior and study the long-term effect of ivermectin on malaria transmission experiments in Kenya. We hope that our work will provide theoretical guidance for the control of malaria transmission using ivermectin in the future.

The rest of this article is structured as follows. In Section 2, we derive a delay malaria transmission model with seasonality a and ivermectin, and present some properties, such as positivity and boundedness of solutions. The basic reproduction ratio R_0 is discussed and use R_0 to analyze the threshold dynamics of the model in Section 3. In Section 4, we demonstrate the validity of our theory by examining the long- term behavior of malaria transmission in Kenya and present an analysis of the effect of ivermectin for malaria control. Finally, in Section 5, a brief summary and discussion are given.

2. Model Formulation

In this section, we propose a seasonal effect of delay malaria transmission model taking into account the treatment and ivermectin. First, we denote the total population size of humans and mosquitoes by $N_h(t)$ and $N_v(t)$, respectively. We classify the human population into five subclasses: susceptible $S_h(t)$, exposed $E_h(t)$, infectious $I_h(t)$, treated $T_h(t)$ and recovered $R_h(t)$ (those who recovered through treatment or recovered naturally, of which they were still slightly infectious). Mosquito

populations are divided into two categories: susceptible $S_v(t)$ and infectious $I_v(t)$. Meanwhile, the time *Plasmodium* in completing its development in the mosquito and migrate to the salivary glands, known as the external incubation period (EIP). Let τ be the length of the EIP. Thus,

$$\begin{aligned} N_h(t) &= S_h(t) + E_h(t) + I_h(t) + T_h(t) + R_h(t), \\ N_v(t) &= S_v(t) + I_v(t-\tau). \end{aligned} \tag{2.1}$$

If a susceptible human S_h is bitten by an infectious mosquito, then the human progresses through the exposed E_h, infectious I_h. The infected humans enter the recovery class R_h either through natural recovery or treatment. However, recovered humans becomes susceptible after losing immunity. Susceptible mosquitoes S_v become infected when they bite infectious, treated or recovered humans, and once infected they move into infectious class I_v. Then, the infection rates per susceptible human is

$$c\beta(t)\frac{N_v(t)}{N_h(t)}\frac{I_v(t)}{N_v(t)} = c\beta(t)\frac{I_v(t)}{N_h(t)},$$

where c is the probability of a mosquito infecting a human, $\beta(t)$ represents the average number of bites per mosquito at time t. By the same idea of model formulation as in [3], we see that the number of newly occurred infectious mosquitoes at time t is given by

$$b\beta(t-\tau)\frac{I_h(t-\tau) + \sigma_1 T_h(t-\tau) + \sigma_2 R_h(t-\tau)}{N_h(t-\tau)} S_v(t-\tau) e^{\int_{t-\tau}^{t} \mu_v(s)\mathrm{d}s},$$

where b is the probability of a human infecting a mosquito, σ_1 is the ratio between the probability of transmission from a treated person to a susceptible mosquito and the probability of transmission from an infected person and σ_2 is the ratio between the probability of transmission from a recovered person to a susceptible mosquito and the probability of transmission from an infected person. $\mu_v(t)$ represents natural mortality rate of mosquitoes.

Mosquitoes leave the total population through natural death and death caused by ivermectin. Mosquito mortality due to ivermectin is mainly determined by vaccination rate of ivermectin and the concentration of ivermectin [24]. Clinical trials investigating have shown that three doses of 300 $\mu g/kg$ given over 3 days has a mosquitocidal effect in humans for 28 days against *Anopheles gambiae* sensu stricto [25]. Therefore, we suppose that the mosquito mortality due to ivermectin is a monthly periodic function, which is denoted by $d_v(t)$. Let κ be the vaccination rate of ivermectin. Then the mosquito mortality due to ivermectin can be described as

$$d_v(t)\beta(t)\frac{\kappa N_h(t)}{N_h(t)} = d_v(t)\kappa\beta(t).$$

Following the above assumptions, we obtain the transmission diagram, see Figure 1:

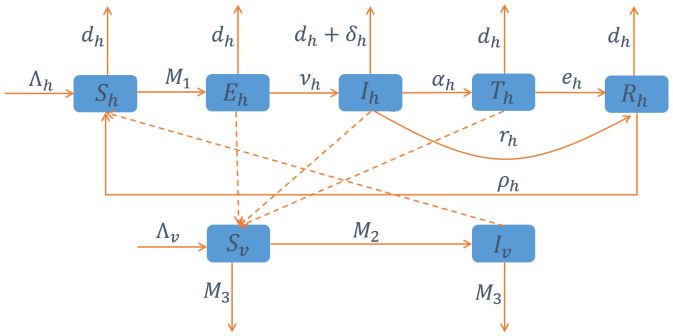

FIGURE 1. Transmission diagram of malaria among human and mosquito. Here $M_1 = c\beta\frac{I_v(t)}{N_h(t)}$, $M_2 = b\beta(t-\tau)\frac{I_h(t-\tau)+\sigma_1 T_h(t-\tau)+\sigma_2 R_h(t-\tau)}{N_h(t-\tau)}S_v(t-\tau)e^{-\int_{t-\tau}^{t}\mu_v(s)\mathrm{dz}}$ and $M_3 = d_v(t)\kappa\beta(t)+\mu_v(t)$.

Accordingly, we obtain the following malaria transmission model with time delay

$$\begin{aligned}
\frac{\mathrm{d}S_h(t)}{\mathrm{d}t} &= \Lambda_h + \rho_h R_h(t) - d_h S_h(t) - c\beta(t)\frac{I_v(t)}{N_h(t)}S_h(t),\\
\frac{\mathrm{d}E_h(t)}{\mathrm{d}t} &= c\beta(t)\frac{I_v(t)}{N_h(t)}S_h(t) - d_h E_h(t) - \nu_h E_h(t),\\
\frac{\mathrm{d}I_h(t)}{\mathrm{d}t} &= \nu_h E_h(t) - d_h I_h(t) - \delta_h I_h(t) - \gamma_h I_h(t) - \alpha_h I_h(t),\\
\frac{\mathrm{d}T_h(t)}{\mathrm{d}t} &= \alpha_h I_h(t) - d_h T_h(t) - e_h T_h(t),\\
\frac{\mathrm{d}R_h(t)}{\mathrm{d}t} &= \gamma_h I_h(t) + e_h T_h(t) - d_h R_h(t) - \rho_h R_h(t),\\
\frac{\mathrm{d}S_v(t)}{\mathrm{d}t} &= \Lambda_v(t) - b\beta(t)\frac{H(t)}{N_h(t)}S_v(t) - d_v(t)\kappa\beta(t)S_v(t) - \mu_v(t)S_v(t),\\
\frac{\mathrm{d}I_v(t)}{\mathrm{d}t} &= b\beta(t-\tau)\frac{H(t-\tau)}{N_h(t-\tau)}S_v(t-\tau)e^{-\int_{t-\tau}^{t}\mu_v(s)\mathrm{ds}} - d_v(t)\kappa\beta(t)I_v(t)\\
&\quad - \mu_v(t)I_v(t),
\end{aligned} \tag{2.2}$$

where $\Lambda_v(t)$, $\beta(t)$, $\mu(t)$ are positive 12-month periodic continuous function. It is easy to see that $e^{-\int_{t-\tau}^{t}\mu_v(s)\mathrm{ds}}$ is positive 12-month periodic function and $H(t) = I_h(t)+\sigma_1 T_h(t)+\sigma_2 R_h(t)$. Explicit description of the parameters of model (2.2) are given in Table 1.

2.1. **Positivity and boundedness of solutions.** Let $C := C\left([-\tau,0],\mathbb{R}^7\right)$, $C^+ = C\left([-\tau,0],\mathbb{R}^7_+\right)$. Define $\|\phi\| = \sum_{i=1}^{7}\|\phi_i\|_\infty$, where $\|\phi_i\|_\infty = \max_{-\tau\le\theta\le 0}|\phi_i(\theta)|$ and $\phi = (\phi_1,\phi_2,\phi_3,\phi_4,\phi_5,\phi_6,\phi_7) \in C$. Then, (C, C^+) is an ordered Banach space , and C^+ is an internally non-empty normal cone of C. For any given continuous function $u : [-\tau,\sigma_\phi) \to \mathbb{R}^7$ with $\sigma_\phi > 0$, we define $u_t \in C$ for $t \ge 0$ by $u_t(\theta) = u(t+\theta)$ for all $\theta \in [-\tau, 0]$.

TABLE 1. Biological description of model (2.2) parameters.

Parameters	Biological significance
Λ_h	Recruitment rate for human population
ρ_h	The probability of moving from recovered to susceptible
d_h	Natural death rate for humans
c	Transmission probability of malaria from mosquitoes to susceptible humans
$\beta(t)$	Biting rate of mosquitoes
ν_h	The transmission rate of humans from the exposed state to the infectious state
δ_v	Malaria death rate for humans
γ_h	The probability of natural recovery of infectious humans rehabilitation
α_h	The probability of infectious population receiving treatment
e_h	Probability of recovery by receiving treatment
$\Lambda_v(t)$	Recruitment rate for mosquitoes population
b	Transmission probability of malaria from humans to susceptible mosquitoes
σ_1	Ratio between the probability of transmission from a treated person to a susceptible mosquito and the probability of transmission from an infected person
σ_2	Ratio between the probability of transmission from a recovered person to a susceptible mosquito and the probability of transmission from an infected person
$d_v(t)$	Ivermectin-induced mortality of mosquitoes
κ	Ivermectin vaccination rate
$\mu_v(t)$	Natural mortality rate of mosquitoes
τ	The time required for *Plasmodium* to develop and mature in mosquitoes

Lemma 2.1. *For any $\phi \in C^+$, model (2.2) has a unique non-negative solution $u(t,\phi)$ with $u(0,\phi) = u_0 = \phi$ such that $u_t(\phi) \in C^+$ on $t \in [0,\infty)$, and all solutions are ultimately bounded.*

Proof. For any $\phi = (\phi_1, \phi_2, \phi_3, \phi_4, \phi_5, \phi_6, \phi_7) \in C^+$, system (2.2) can be written as

$$\begin{aligned} \dot{u} &= f(t,u), \\ u(0,\phi) &= \phi, \end{aligned} \tag{2.3}$$

where the vector field $f(t,u)$ is generated by the right side of system (2.2). Since $f(t,u)$ is continuous in $(t,u) \in \mathbb{R}_+ \times C^+$ and Lipschitz in u on each compact subset of $\mathbb{R}\times C^+$, so it then follows from [11, Theorems 2.2.1 and 2.2.3] that model (2.2) has a unique solution $u(t,\phi)$ with $u_0 = \phi$ on its maximum interval $[0,\sigma_\phi)$ of existence.

For any $\phi \in C^+$ with $\phi_i(0) = 0$, it is obvious that $f_i(t,\phi) \geq 0$ for i=1,2,3,4,5,6,7. By [26, Theorem 5.2.1 and Remark 5.2.1], the unique solution $u(t,\phi)$ of model (2.2) with $u_0 = \phi$ satisfies $u_t(\phi) \in C^+$ for all $t \in [0,\sigma_\phi)$.

From the first equation of (2.1) and model (2.2), we have

$$\begin{aligned}
\frac{\mathrm{d}N_h(t)}{\mathrm{d}t} &= \Lambda_h - d_h N_h(t) - \delta_h I_h(t) \le \Lambda_h - d_h N_h(t),\\
\frac{\mathrm{d}S_v(t)}{\mathrm{d}t} &\le \Lambda_v(t) - d_v(t)\kappa\beta(t)S_v(t) - \mu_v(t)S_v(t),\\
\frac{\mathrm{d}I_v(t)}{\mathrm{d}t} &\le b\beta(t-\tau)S_v(t-\tau) - d_v(t)\kappa\beta(t)I_v(t) - \mu_v(t)I_v(t),
\end{aligned} \tag{2.4}$$

when $t \in [0, \sigma_\phi)$. Thus, $S_h(t)$, $E_h(t)$, $I_h(t)$, $T_h(t)$, $R_h(t)$, $S_v(t)$, $I_v(t)$ are bounded on $[0, \sigma_\phi)$, which implies that $\sigma_\phi \to \infty$ by [11, Theorem 2.3.1].

Note that the linear equation $\frac{\mathrm{d}\hat{N}_h(t)}{\mathrm{d}t} = \Lambda_h - d_h\hat{N}_h(t)$ has a globally stable equilibrium point $\hat{N}_h^* = \frac{\Lambda_h}{d_h}$, it follows from the comparison principle that

$$\limsup_{t\to\infty} \left(S_h(t) + E_h(t) + I_h(t) + T_h(t) + R_h(t)\right) \le \hat{N}_h^* = \frac{\Lambda_h}{d_h}.$$

This means that $S_h(t), E_h(t), I_h(t), T_h(t), R_h(t)$ are ultimately bounded. Similarly, we have $S_v(t)$ is ultimately bounded by the second inequation of (2.4).

Let

$$g^h = \max_{t>\tau} g(t) \quad \text{and} \quad g^l = \min_{t>\tau} g(t),$$

where $g(t)$ is any bounded function on $[\tau, \infty)$. From the seventh equation of model (2.2), we have

$$\frac{\mathrm{d}I_v(t)}{\mathrm{d}t} \le b\beta^h S_v^h - \left(d_v^l\kappa\beta^l + \mu_v^l\right) I_v(t),$$

Then, $I_v(t)$ is ultimately bounded for $t > \tau$. This implies that all solutions of the model (2.2) are ultimately bounded. □

3. Threshold dynamics

3.1. **Basic reproduction ratios.** To deduce the basic reproduction ratio R_0 for the model (2.2), we need to find the disease-free state of the model (2.2). Let $E_h = I_h = T_h = R_h = I_v = 0$, we obtain

$$\begin{aligned}
\frac{\mathrm{d}S_h(t)}{\mathrm{d}t} &= \Lambda_h - d_h S_h(t),\\
\frac{\mathrm{d}S_v(t)}{\mathrm{d}t} &= \Lambda_v(t) - d_v(t)\kappa\beta(t)S_v(t) - \mu_v(t)S_v(t).
\end{aligned} \tag{3.1}$$

Model (3.1) has a unique positive disease-free periodic solution

$$E_0 = (S_h^*, 0, 0, 0, 0, 0, S_v^*(t), 0),$$

where $S_h^* = \frac{\Lambda_h}{d_h}$, and

$$\begin{aligned}
S_v^*(t) = \Big[\int_0^t \Lambda(r) e^{\int_0^r d_v(s)\kappa\beta(s) + \mu_v(s)\mathrm{d}s}\mathrm{d}r + \frac{\int_0^\omega \Lambda(r) e^{\int_0^r d_v(s)\kappa\beta(s)+\mu_v(s)\mathrm{d}s}\mathrm{d}r}{e^{\int_0^\omega d_v(r)\kappa\beta(r)+\mu_v(r)\mathrm{d}r} - 1}\Big]\\
\times e^{-\int_0^t d_v(r)\kappa\beta(r)+\mu_v(r)\mathrm{d}r}.
\end{aligned}$$

Following the basic reproduction ratio theory developed by [34], we first linearize model (2.2) at the disease-free periodic solution E_0, then we obtain

$$\begin{aligned}
\frac{\mathrm{d}E_h(t)}{\mathrm{d}t} &= c\beta(t)I_v(t) - \tilde{a}E_h(t),\\
\frac{\mathrm{d}I_h(t)}{\mathrm{d}t} &= \nu_h E_h(t) - \tilde{b}I_h(t),\\
\frac{\mathrm{d}T_h(t)}{\mathrm{d}t} &= \alpha_h I_h(t) - \tilde{c}T_h(t),\\
\frac{\mathrm{d}R_h(t)}{\mathrm{d}t} &= \gamma_h I_h(t) + e_h T_h(t) - \tilde{d}R_h(t),\\
\frac{\mathrm{d}I_v(t)}{\mathrm{d}t} &= b\beta(t-\tau)\frac{H(t-\tau)}{S_h^*}S_v^*(t-\tau)e^{-\int_{t-\tau}^{t}\mu_v(s)\mathrm{d}s} - \tilde{g}(t)I_v(t),
\end{aligned} \tag{3.2}$$

where $\tilde{a} = d_h + \nu_h$, $\tilde{b} = d_h + \delta_h + \gamma_h + \alpha_h$, $\tilde{c} = d_h + e_h$, $\tilde{d} = d_h + \rho_h$, $\tilde{g}(t) = d_v(t)\kappa\beta(t) + \mu_v(t)$.

Let $\bar{C} := C([-\tau, 0], \mathbb{R}^5)$ and $\bar{C}^+ := C([-\tau, 0], \mathbb{R}^5_+)$, then $(\bar{C}, \bar{C}^+)$ is an ordered Banach space. Let $F : \mathbb{R} \to \mathcal{L}(C, \mathbb{R}^5)$ be a map and $V(t)$ be a 5×5 matrix function on $\mathbb{R}$. For any $t \in \mathbb{R}$ and $\phi = (\phi_1, \phi_2, \phi_3, \phi_4, \phi_5)^T \in \bar{C}$, one has

$$F(t)\phi = \begin{pmatrix} c\beta(t)\phi_5(0) \\ 0 \\ 0 \\ 0 \\ b\beta(t-\tau)\frac{I_h(-\tau)+\sigma_1 T_h(-\tau)+\sigma_2 R_h(-\tau)}{S_h^*}S_v^*(t-\tau)e^{-\int_{t-\tau}^{t}\mu_v(s)\mathrm{d}s} \end{pmatrix}$$

and

$$V(t) = \begin{pmatrix} \tilde{a} & 0 & 0 & 0 & 0 \\ -\nu_h & \tilde{b} & 0 & 0 & 0 \\ 0 & -\alpha_h & \tilde{c} & 0 & 0 \\ 0 & -\gamma_h & -e_h & \tilde{d} & 0 \\ 0 & 0 & 0 & 0 & \tilde{g}(t) \end{pmatrix}.$$

Then the linear system (3.2) can be written as

$$\frac{\mathrm{d}u(t)}{\mathrm{d}t} = (F(t) - V(t))u(t), \quad t \geq 0,$$

where $u(t) = (E_h(t), I_h(t), T_h(t), R_h(t), I_v(t))^T$. The internal evolution of individuals in the infectious compartments is governed by the linear ordinary differential system:

$$\frac{\mathrm{d}u}{\mathrm{d}t} = -V(t)u(t).$$

Let $\Phi(t, s)$, $t \geq s$, be the evolution matrix of the above linear system. For each $s \in \mathbb{R}$, $\Phi(t, s)$ satisfies

$$\frac{\mathrm{d}\Phi(t,s)}{\mathrm{d}t} = -V(t)\Phi(t,s), \quad t \geq s \text{ and } \Phi(s,s) = I,$$

where I is the 5×5 identity matrix. It then follows that

$$\Phi(t,s)=\begin{pmatrix} e^{-\tilde{a}(t-s)} & 0 & 0 & 0 & 0\\ a_{21}e^{-\tilde{b}(t-s)} & e^{-\tilde{b}(t-s)} & 0 & 0 & 0\\ a_{31}e^{-\tilde{c}(t-s)} & a_{32}e^{-\tilde{c}(t-s)} & e^{-\tilde{c}(t-s)} & 0 & 0\\ a_{41}e^{-\tilde{d}(t-s)} & a_{42}e^{-\tilde{d}(t-s)} & a_{43}e^{-\tilde{d}(t-s)} & e^{-\tilde{d}(t-s)} & 0\\ 0 & 0 & 0 & 0 & e^{-\int_s^t \tilde{g}(\xi)\mathrm{d}\xi} \end{pmatrix},$$

where $a_{21}=\nu_h(t-s)$, $a_{31}=\frac{1}{2}\alpha_h\nu_h(t-s)^2$, $a_{32}=\alpha_h(t-s)$, $a_{41}=\frac{1}{6}\alpha_h\nu_h e_h(t-s)^3+\frac{1}{2}\gamma_h\nu_h(t-s)^2$, $a_{42}=\frac{1}{2}\alpha_h e_h(t-s)^2+\gamma_h(t-s)$ and $a_{43}=e_h(t-s)$.

Let C_ω be the ordered Banach space of all ω-periodic continuous functions from $\mathbb{R}$ to $\mathbb{R}^5$, and equipped with the maximum norm $\|.\|_\infty$ and the positive cone $C_\omega^+:=\{\upsilon\in C_\omega:\upsilon(t)\geq 0,\text{for } t\in\mathbb{R}\}$. We suppose that $\upsilon(s)\in C_\omega$ is the initial distribution of infectious individuals in this periodic environment. Then for any given $s\geq 0$, $F(t-s)\upsilon_{t-s}$ is the distribution of newly infected individuals at time $t-s$, which is produced by the infectious individuals who were introduced over the time interval $[t-s-\tau,t-s]$. Then $\Phi(t,t-s)F(t-s)\upsilon_{t-s}$ is the distribution of those infected individuals who were newly infected at time $t-s$ and remain in the infected compartments at time t. It follows that

$$\int_0^\infty \Phi(t,t-s)F(t-s)\upsilon_{t-s}\mathrm{d}s=\int_0^\infty \Phi(t,t-s)F(t-s)\upsilon(t-s+\cdot)\mathrm{d}s$$

is the distribution of accumulative new infections at time t produced by all those infected individuals $\upsilon(s)$ introduced at the previous time to t. We define a linear operator $L:C_\omega\to C_\omega$ as follows

$$[L\upsilon](t)=\int_0^{+\infty}\Phi(t,t-s)F(t-s)\upsilon(t-s+\cdot)\mathrm{d}s,\quad \text{for any } t\in\mathbb{R},\ \upsilon\in C_\omega,$$

where L is called the next infection operator. It then follows from [34] that the basic reproduction ratio R_0 for system (3.2) is defined as the spectral radius of operator L, that is $R_0=\rho(L)$.

For a given $t\geq 0$, let $P(t)$ be the solution maps of system (3.2), that is $P(t)\phi=v_t(\phi)=v(t,\phi)$, where $v(t,\phi)$ is the unique solution of system (3.2) with $v_0=\phi\in C$. Then $P:=P(\omega)$ is the Poincaré map associated with system (3.2). Let $r(P)$ be the spectral radius of P. By [34, Theorem 2.1], we have the following result.

Lemma 3.1. *R_0-1 has the same sign as $r(P)-1$.*

To study the relationship between the global properties of system (3.2) and R_0, we need to prove the existence of the exponential positive solution of system (3.2). For this purpose, we first define a phase space:

$$Y:=R\times[C((-\tau,0),\mathbb{R})]^3\times R,$$
$$Y^+:=R\times[C((-\tau,0),\mathbb{R}_+)]^3\times R.$$

Similar to the proof of Lemma 2.1, we can obtain the following result.

Lemma 3.2. *For a $\phi\in Y^+$, system (3.2) has a unique non-negative solution $v(t,\phi)\in Y^+$ with $v_0=\phi$ for all $t\geq 0$.*

For a given $t\geq 0$, let $\hat{P}(t)$ be the solution maps of system (3.2) on Y. The following lemma indicates that that the periodic semi-flow $\hat{P}(t)$ is eventually strongly positive.

Lemma 3.3. *For $\phi \in Y^+ \setminus \{\mathbf{0}\}$, the solution $v(t,\phi)$ with $v_0 = \phi$ of system (3.2) satisfies $v_i(t,\phi) > 0$ for all $t > \tau$, $i = 1,2,3,4,5$ and hence, $\hat{P}(t)\phi \gg 0$ for all $t > \tau$.*

Proof. For a given $\phi = (\phi_1, \phi_2, \phi_3, \phi_4, \phi_5) \in Y^+ \setminus \{\mathbf{0}\}$, let

$$v(t,\phi) = (v_1(t), v_2(t), v_3(t), v_4(t), v_5(t)).$$

If $v_1(0) > 0$, by solving system (3.2), for all $t > 0$, we obtain

$$v_1(t) = e^{-\tilde{a}t}\Big(v_1(0) + \int_0^t c\beta(\xi)v_5(\xi)e^{\tilde{a}\xi}\mathrm{d}\xi\Big) \geq e^{-\tilde{a}t}v_1(0) > 0,$$

$$v_2(t) = e^{-\tilde{b}t}\Big(v_2(0) + \int_0^t \nu_h v_1(\xi)e^{\tilde{b}\xi}\mathrm{d}\xi\Big) \geq e^{-\tilde{b}t}\Big(\int_0^t \nu_h v_1(\xi)e^{\tilde{b}\xi}\mathrm{d}\xi\Big) > 0.$$

Similarly, we can obtain in turn

$$v_3(t) = e^{-\tilde{c}t}\Big(v_3(0) + \int_0^t \alpha_h v_2(\xi)e^{\tilde{c}\xi}\mathrm{d}\xi\Big) > 0,$$

$$v_4(t) = e^{-\tilde{d}t}\Big(v_4(0) + \int_0^t (e_h + \gamma_h)v_3(\xi)e^{\tilde{d}\xi}\mathrm{d}\xi\Big) > 0,$$

When $t > \tau$, we find that

$$\begin{aligned} v_5(t) &= e^{-\int_0^t \tilde{g}(\xi)\mathrm{d}\xi}v_5(0) \\ &\quad + e^{-\int_0^t \tilde{g}(\xi)\mathrm{d}\xi}\int_0^t b\beta(\xi-\tau)\frac{H_h(\xi-\tau)}{S_h^*}S_v^*(\xi-\tau)e^{-\int_{\xi-\tau}^{\xi}\mu_v(z)\mathrm{d}z}e^{\int_0^{\xi}\mu_v(z)\mathrm{d}z}\mathrm{d}\xi \\ &\quad > 0. \end{aligned}$$

That implies

$$(v_1(t), v_2(t), v_3(t), v_4(t), v_5(t)) > (0,0,0,0,0) \quad \text{for all } t > \tau. \tag{3.3}$$

By similar discussion, we obtain (3.3) when $v_i(0) > 0$ for $i = 2,3,4,5$. Then we obtain $\hat{P}(t)$ is strongly positive on Y^+ for $t > \tau$. □

Furthermore, $\hat{P} := \hat{P}(\omega)$ is the Poincaré map associated with system (3.2). Let $r(\hat{P})$ be the spectral radius of $\hat{P}$. Choose an integer $n_0 > 0$ such that $n_0\omega > \tau$. By Lemma 3.3, we see that $\hat{P}^{n_0} = \hat{P}(n_0\omega)$ is strongly positive. Following [11, Theorem 3.6.1], the linear operator $\hat{P}^{n_0}$ is compact on Y^+. Since $r(\hat{P}^{n_0}) = r(\hat{P})^{n_0}$ and according to the Krein-Rutman theorem, we obtain that $r(\hat{P})$ is a simple eigenvalue and having a strongly positive eigenvector. By [13, Lemma 3.8], we have $r(P) = r(\hat{P})$. From [35], we have the following result.

Lemma 3.4. *Let $\mu = \frac{\ln r(P)}{\omega}$. Then there exists a positive ω-periodic function $v^*(t)$ such that $u^*(t) = e^{\mu t}v^*(t)$ is a positive solution of linear system (3.2).*

3.2. **Equilibrium stability.** In this part, we establish a threshold-type result on the global dynamics of model (2.2) in terms of R_0. Let

$$X := C([-\tau, 0], \mathbf{R}_+^7),$$

$$X_0 := \{\phi \in X : \phi_i(0) > 0 \text{ for any } i \in 2,3,4,5,7\},$$

$$\partial X_0 := X \backslash X_0 = \{\phi \in X : \phi_2(0)\phi_3(0)\phi_4(0)\phi_5(0)\phi_7(0) = 0\},$$

where $\phi = (\phi_1, \phi_2, \phi_3, \phi_4, \phi_5, \phi_6, \phi_7)$.

Theorem 3.5. *If $\mathcal{R}_0 > 1$, then model (2.2) exists a positive ω -periodic solution, and there exist a positive real number $\eta > 0$ such that the solution $(S_h(t), E_h(t), I_h(t), T_h(t), R_h(t), S_v(t), I_v(t)) \in X$ with $S_h(0) > 0, E_h(0) > 0, I_h(0) > 0, T_h(0) > 0, R_h(0) > 0, S_v(0) > 0, I_v(0) > 0$ satisfies*

$$\liminf_{t\to\infty} (E_h(t), I_h(t), T_h(t), R_h(t), I_v(t)) \geq (\eta, \eta, \eta, \eta, \eta).$$

Proof. Let $Q(t) : X \to X$ be the solution maps of model (2.2), that is $Q(t)\phi = u(t, \phi) = u_t(\phi)$, $t \geq 0$, where $u(t, \phi)$ is the unique solution of the model (2.2) with $u_0 = \phi \in X$. Then $Q := Q(\omega)$ is the Poincaré map associated with model (2.2), and $Q^n = Q(n\omega)$. It is easy to find that $Q(t)\,(X_0) \subset X_0$ for all $t \geq 0$. Now, we prove that $Q(t)$ is uniformly persistent with respect to $(X_0, \partial X_0)$.

Let $M_1 = (S_h^*, 0, 0, 0, 0, S_{v0}^*, 0)$, where $S_{v0}^*(\theta) = S_v^*(\theta)$ for $\theta \in [-\tau, 0]$. Then $Q(t)M_1 = M_1$ for all $t \geq 0$. Since $\lim_{\phi\to M_1} \|Q(t)\phi - Q(t)M_1\| = 0$ uniformly for $t \in [0, \omega]$, for any given $\varepsilon > 0$, there exists a positive real number $\delta = \delta(\varepsilon)$ such that for any ϕ satisfying $\|\phi - M_1\| < \delta$, we have

$$\|Q(t)\phi - Q(t)M_1\| \leq \varepsilon, \quad \text{for } t \in [0, \omega].$$

We proceed with the following two claims.

Claim 1. $\limsup_{n\to\infty} \|Q^n(\phi) - M_1\| \geq \delta$ for all $\phi \in X_0$. Suppose by contradiction that $\limsup_{n\to\infty} \|Q^n(\psi) - M_1\| < \delta$ for some $\psi \in X_0$. Then, there exists an integer $N \geq 1$ such that$\|Q^n(\psi) - M_1\| < \delta$ for all $n \geq N$. For any $t \geq N\omega$, letting $t = n\omega + t'$ with $n \geq N$ and $t' \in [0, \omega)$, we have

$$\|Q(t)\psi - Q(t)M_1\| = \|Q(t')(Q^n(\psi)) - Q(t')M_1\| < \varepsilon.$$

Then for all $t \geq N\omega$,

$$S_h^* - \varepsilon < S_h(t, \psi) < S_h^* + \varepsilon, \quad S_v^*(t) - \varepsilon < S_v(t, \psi) < S_v^*(t) + \varepsilon,$$
$$0 < E_h(t, \psi),\ I_h(t, \psi),\ T_h(t, \psi),\ R_h(t, \psi),\ I_v(t, \psi) < \varepsilon.$$

We also have the inequalities

$$\frac{S_h(t, \psi)}{N_h(t, \psi)} \geq \frac{S_h^* - \varepsilon}{S_h^* + 5\varepsilon} = 1 - \frac{6\varepsilon}{S_h^* + 5\varepsilon} \quad \text{and} \quad \frac{S_v(t, \psi)}{N_h(t, \psi)} \geq \frac{S_v^*(t) - \varepsilon}{S_h^* + 5\varepsilon}.$$

Then from model (2.2), for $t \geq N\omega + \tau$, we have

$$\begin{aligned}
\frac{\mathrm{d}E_h(t)}{\mathrm{d}t} &\geq c\beta(t)\left(1 - \frac{6\varepsilon}{S_h^* + 5\varepsilon}\right) I_v(t) - (d_h + \nu_h)E_h(t),\\
\frac{\mathrm{d}I_h(t)}{\mathrm{d}t} &= \nu_h E_h(t) - (d_h + \delta_h + \gamma_h + \alpha_h)\, I_h(t),\\
\frac{\mathrm{d}T_h(t)}{\mathrm{d}t} &= \alpha_h I_h(t) - (d_h + e_h)T_h(t),\\
\frac{\mathrm{d}R_h(t)}{\mathrm{d}t} &= \gamma_h I_h(t) + e_h T_h(t) - (d_h - m)R_h(t),\\
\frac{\mathrm{d}I_v(t)}{\mathrm{d}t} &\geq b\beta(t-\tau)\frac{H(t-\tau)}{S_h^* + 5\varepsilon}(S_v^*(t-\tau) - \varepsilon)e^{-\int_{t-\tau}^{t}\mu_v(s)\mathrm{d}z}\\
&\quad - (d_v(t)\kappa\beta(t) + \mu_v(t))I_v(t).
\end{aligned} \tag{3.4}$$

Let P_ε be the solution map of the perturbed linear periodic system

$$\begin{aligned}
\frac{\mathrm{d}\bar{E}_h(t)}{\mathrm{d}t} &= c\beta(t)\left(1-\frac{6\varepsilon}{S_h^*+5\varepsilon}\right)\bar{I}_v(t)-(d_h+\nu_h)\bar{E}_h(t),\\
\frac{\mathrm{d}\bar{I}_h(t)}{\mathrm{d}t} &= \nu_h\bar{E}_h(t)-(d_h+\delta_h+\gamma_h+\alpha_h)\bar{I}_h(t),\\
\frac{\mathrm{d}\bar{T}_h(t)}{\mathrm{d}t} &= \alpha_h\bar{I}_h(t)-(d_h+e_h)\bar{T}_h(t),\\
\frac{\mathrm{d}\bar{R}_h(t)}{\mathrm{d}t} &= \gamma_h\bar{I}_h(t)+e_h\bar{T}_h(t)-(d_h+m)\bar{R}_h(t),\\
\frac{\mathrm{d}\bar{I}_v(t)}{\mathrm{d}t} &= b\beta(t-\tau)\frac{\bar{H}(t-\tau)}{S_h^*+5\varepsilon}(S_v^*(t-\tau)-\varepsilon)e^{-\int_{t-\tau}^{t}\mu_v(s)\mathrm{d}z}\\
&\quad-(d_v(t)\kappa\beta(t)+\mu_v(t))\bar{I}_v(t),
\end{aligned}$$

with $P_\varepsilon := P_\varepsilon(\omega)$. Since $R_0>1$, $\lim_{\varepsilon\to 0^+} r(P_\varepsilon)=r(P)>1$, there exists a sufficiently small $\varepsilon>0$ such that $\varepsilon<\min\{\min_{t\in[0,\omega]}S_v^*(t),S_h^*\}$ and $r(P_\varepsilon)>1$. By Lemma 3.4, there is a positive ω-periodic function $v_\varepsilon^*(t)$ such that $\bar{v}_\varepsilon(t)=e^{\lambda t}v_\varepsilon^*(t)$ is a solution of above perturbed linear periodic system, where $\lambda=\frac{\ln r(P_\varepsilon)}{\omega}>0$. Then we have $\bar{v}_\varepsilon(t)\to+\infty$ as $t\to+\infty$. And because of the system (3.4), the comparison principle implies that

$$\lim_{t\to\infty}(E_h(t,\psi),I_h(t,\psi),T_h(t,\psi),R_h(t,\psi),I_h(t,\psi))=(\infty,\infty,\infty,\infty,\infty,\infty),$$

which leads to a contradiction.

By claim 1 above, we can see that M_1 is an isolated invariant set for Q in X, and $W^s(M_1)\cap X_0=\emptyset$, where $W^s(M_1)$ is the stable set of M_1 for Q.

Claim 2. $M_\partial=\{\phi\in\partial X_0:\phi_i(0)=0,\ i=2,3,4,5,7\}$, where $M_\partial:=\{\phi\in\partial X_0:Q^n(\phi)\in\partial X_0,\text{for } n\geq 0\}$. Clearly, it suffices to prove that for any $\varphi\in M_\partial$,

$$(E_h(t,\varphi),I_h(t,\varphi),T_h(t,\varphi),R_h(t,\varphi),I_h(t,\varphi))=(0,0,0,0,0)$$

holds for all $t\geq 0$. Suppose not, then there exists some $t_0\geq 0$ such that $E_h(t_0,\varphi)>0$ or $I_h(t_0,\varphi)>0$ or $T_h(t_0,\varphi)>0$ or $R_h(t_0,\varphi)>0$ or $I_v(t_0,\varphi)>0$.

Assuming that $E_h(t_0,\varphi)>0$, then by the second equation of the model (2.2) we know that $\frac{dE_h}{dt}\geq-(d_h+\nu_h)E_h(t)$ and

$$E_h(t,\varphi)\geq E_h(t_0,\varphi)e^{(d_h+\nu_h)(t_0-t)}>0,\quad\text{for}\quad t>t_0.$$

Following the third equation of the model (2.2) we know that

$$I_h(t,\varphi)>\int_{t_0}^{t}\nu_hE_h(s,\varphi)e^{(s-t)(d_h+\delta_h+\gamma_h+\alpha_h)}\mathrm{d}s>0,\quad\text{for all } t>t_0.$$

By the same argument, $T_h(t,\varphi)>0$ and $R_h(t,\varphi)>0$ for any $t>t_0$. Similar, it is easy to see that

$$I_v(t,\varphi)>\int_{t_0}^{t}b\beta(s-\tau)\frac{H(s-\tau,\varphi)}{N_h(s-\tau)}S_v(s-\tau,\varphi)e^{\int_{s-\tau}^{s}\mu(z)\mathrm{d}z}e^{\int_t^s(d_v\kappa\beta(z)+\mu(z))\mathrm{d}z}\mathrm{d}s>0,$$

when $t>t_0+\tau$, where $N_h(s-\tau)=S_h(s-\tau,\varphi)+E_h(s-\tau,\varphi)+I_h(s-\tau,\varphi)+T_h(s-\tau,\varphi)+R_h(s-\tau,\varphi)$. Thus, $(E_h(t,\varphi),I_h(t,\varphi),T_h(t,\varphi),R_h(t,\varphi),I_h(t,\varphi))>(0,0,0,0,0)$ for all $t>t_0+\tau$. Then we can find some $n>0$ with $n\omega>t_0+\tau$ such that

$$(E_h(n\omega,\varphi),I_h(n\omega,\varphi),T_h(n\omega,\varphi),R_h(n\omega,\varphi),I_h(n\omega,\varphi))\notin M_\partial$$

for all $t > t_0 + \tau$, which is a contradiction.

Similarly, when $I_h(0) > 0$ or $T_h(0) > 0$ or $R_h(0) > 0$ or $I_v(0) > 0$, we can obtain the same contradiction. Therefore, Claim 2 is proved. Moreover, from system (3.1), we have $S_h(t,\phi) \to S_h^*$, $S_v(t,\phi) \to S_v^*(t)$ as $t \to \infty$, i.e., $Q^n(\phi) \to M_1$. Thus, $cup_{\psi \in M_\partial} \omega(\psi) = \{M_1\}$. That means M_1 cannot form a cycle in ∂X_0.

By Claims 1 and 2 and the acyclicity theorem on uniform persistence for maps [35, Theorem 1.3.1 and Remark 1.3.1], it follows that $Q : X \to X$ is uniformly persistent with respect to $(X_0, \partial X_0)$.

We can prove the practical uniform persistence, that is, there exists an $\eta > 0$ such that

$$\liminf_{t\to\infty} \min(E_h(t,\phi), I_h(t,\phi), T_h(t,\phi), R_h(t,\phi), I_v(t,\phi)) = \liminf_{t\to\infty} p(Q(t)\phi) \geq \eta,$$

for all $\phi \in X_0$. The proof is quite standard, a more detailed display of a similar reasoning can be found in [12]. □

Theorem 3.6. *If $R_0 < 1$ and $\delta_h = 0$, the disease-free periodic solution E_0 is globally attractive for model (2.2) in X.*

Proof. In view of model (2.2) and (3.1), there exists a sufficiently large integer $n > 0$ with $n\omega \geq \tau$ and a such that

$$N_h(t) \geq N_h^* - \epsilon = \frac{\Lambda_h}{d_h} - \epsilon, \quad S_v(t) \leq \bar{S}_v^*(t) + \epsilon, \quad \text{for all } t \geq n\omega - \tau.$$

Therefore, for all $t \geq n\omega$, we have

$$\begin{aligned}
\frac{\mathrm{d}E_h(t)}{\mathrm{d}t} &\leq c\beta(t)I_v(t) - (d_h + \nu_h)E_h(t),\\
\frac{\mathrm{d}I_h(t)}{\mathrm{d}t} &= \nu_h E_h(t) - (d_h + \gamma_h + \alpha_h)I_h(t),\\
\frac{\mathrm{d}T_h(t)}{\mathrm{d}t} &= \alpha_h I_h(t) - (d_h + e_h)T_h(t),\\
\frac{\mathrm{d}R_h(t)}{\mathrm{d}t} &= \gamma_h I_h(t) + e_h T_h(t) - (d_h + m)R_h(t),\\
\frac{\mathrm{d}I_v(t)}{\mathrm{d}t} &\leq b\beta(t-\tau)\frac{H(t-\tau)}{N_h^* - \epsilon}(S_v^*(t-\tau) + \epsilon)e^{-\int_{t-\tau}^t \mu_v(s)\mathrm{d}s}\\
&\quad - (d_v(t)\kappa\beta(t) + \mu_v(t))I_v(t).
\end{aligned}$$

Let P_ϵ be the Poincaré map of the auxiliary system

$$\begin{aligned}
\frac{\mathrm{d}\tilde{E}_h(t)}{\mathrm{d}t} &= c\beta(t)\tilde{I}_v(t) - (d_h+\nu_h)\tilde{E}_h(t),\\
\frac{\mathrm{d}\tilde{I}_h(t)}{\mathrm{d}t} &= \nu_h\tilde{E}_h(t) - (d_h+\gamma_h+\alpha_h)\tilde{I}_h(t),\\
\frac{\mathrm{d}\tilde{T}_h(t)}{\mathrm{d}t} &= \alpha_h\tilde{I}_h(t) - (d_h+e_h)\tilde{T}_h(t),\\
\frac{\mathrm{d}\tilde{R}_h(t)}{\mathrm{d}t} &= \gamma_h\tilde{I}_h(t) + e_h\tilde{T}_h(t) - (d_h+m)\tilde{R}_h(t),\\
\frac{\mathrm{d}\tilde{I}_v(t)}{\mathrm{d}t} &= b\beta(t-\tau)\frac{\tilde{H}(t-\tau)}{N_h^*-\epsilon}(S_v^*(t-\tau)+\epsilon)e^{-\int_{t-\tau}^{t}\mu_v(s)\mathrm{d}s}\\
&\quad - (d_v(t)\kappa\beta(t)+\mu_v(t))\tilde{I}_v(t).
\end{aligned} \tag{3.5}$$

Since $\lim_{\epsilon\to 0} r(P_\epsilon) = r(P) < 1$, we fix a sufficiently small $\epsilon \in (0, N_h^*)$ and $r(P_\epsilon) < 1$. In a similar manner, there is a positive ω-periodic function $v_\epsilon^*(t)$ such that $\bar{v}_\epsilon(t) = e^{\lambda t}v_\epsilon^*(t)$ is a positive solution of (3.5), where $\lambda = \frac{\ln r(P_\epsilon)}{\omega} < 0$.

Assuming that $E_0^* = (E_h(t,\psi), I_h(t,\psi), T_h(t,\psi), R_h(t,\psi), I_h(t,\psi))$ is a positive ω-periodic solution of system (3.2). we can choose a sufficiently large constant $K > 0$ such that $E_0^* \le K\bar{v}_\varepsilon(t)$ for all $t \in [n\omega, n\omega+\tau]$. It follows from [26, Theorem 5.1.1], we can get $E_0^* \le K\bar{v}_\varepsilon(t)$, for all $t \ge n\omega+\tau$. Thus, we have $\lim\limits_{t\to\infty} E^* = (E_h(t), I_h(t), T_h(t), R_h(t), I_v(t)) = (0,0,0,0,0)$ when $R_0 < 1$. Meanwhile, we can obtain the following limit system for model (2.2):

$$\begin{aligned}
\frac{\mathrm{d}S_h(t)}{\mathrm{d}t} &= \Lambda_h - d_hS_h(t),\\
\frac{\mathrm{d}S_v(t)}{\mathrm{d}t} &= \Lambda_v(t) - d_v(t)\kappa\beta(t)S_v(t) - \mu_v(t)S_v(t).
\end{aligned}$$

Because S_h^* is globally asymptotically stable and $S_v^*(t)$ is globally attractive, we have

$$\lim_{t\to\infty}\big(S_h(t), E_h(t), I_h(t), T_h(t), R_h(t), S_v(t), I_v(t)\big) = \big(S_h^*, 0, 0, 0, 0, 0, S_v^*(t), 0\big)$$

by the chain transitive sets arguments [35, Theorem 1.2.1]. □

4. Study case

In this section, based on malaria data and clinical trial data of ivermectin in malaria transmission control from Kenya, we estimate the values of parameters related to malaria and invermectin-induced mortality of mosquitoes $d_v(t)$, Then, the numerical fitted curve of malaria transmission cases is shown in Figure 3 and 4. Sensitivity analysis of the ivermectin vaccination rate κ and mosquito bite rate $\beta(t)$, and analysis of the effect of ivermectin vaccination rate, number of and timing between vaccine intervention rounds on malaria transmission control are given in Figure 7 and Figure 11, respectively.

4.1. **Parameter estimation.**

According to the information provided by World Health Organization [28], the total population of Kenya in 2013 is $N_h = 45519986$

and the average life expectancy of humans is 63.419 years. Thus, the human natural death rate d_h can be calculated as follows :

$$d_h = \frac{1}{63.419 \times 12} \approx 0.0013 \quad \text{Month}^{-1}.$$

The recruitment rate Λ_h is:

$$\Lambda_h = d_h \times 45519986 \approx 59813 \quad \text{Humans} \times \text{Month}^{-1}.$$

The values of constant parameters for system (3.2) that do not heavily depend on temperature are listed in Table 2 from [8, 14, 23, 27]. Next, we evaluate the periodic parameters $\mu(t)$ and $\beta(t)$ in system (3.2) by using the monthly mean temperature data from 2002 to 2020 from [29], which is shown in Table 3.

TABLE 2. Parameter values.

parameters	**Values**	**Dimension**	**Sources**
Λ_h	59175	Humans	See text
ρ_h	0.01672	Month^{-1}	[8, 14]
d_h	0.0013	Month^{-1}	See text
c	0.01	Dimensionless	[8]
$\beta(t)$	To be evaluated	Month^{-1}	See text
ν_h	3.344	Month^{-1}	[8]
δ_h	0.002736	Month^{-1}	[8]
α_h	0.53	Dimensionless	[23]
e_h	0.85	Dimensionless	[27]
γ_h	0.13984	Month^{-1}	[8]
$\Lambda_v(t)$	To be evaluated	Month^{-1}	See text
b	0.2	Dimensionless	[8, 14]
σ_1	0.5	Dimensionless	Assumed
σ_2	0.1	Dimensionless	Assumed
$\mu_v(t)$	To be evaluated	Month^{-1}	See text
$d_v(t)$	To be evaluated	Dimensionless	Assumed
κ	[0,1]	Dimensionless	Assumed
τ	9/30.4	Dimensionless	[8]

TABLE 3. Monthly mean temperature of Kenya (in °C).

Month	**Jan.**	**Feb.**	**Mar.**	**Apr.**	**May**	**Jun.**
Temperature	25.50	26.28	26.74	26.11	25.05	24.06
Month	**Jul.**	**Aug.**	**Sep.**	**Oct.**	**Nov.**	**Dec.**
Temperature	23.44	23.83	24.59	25.37	25.08	25.03

It follows from [14] that the temperature dependent mosquito biting rate can be expressed as:

$$\beta(C) = \frac{30.4}{107.204 - 13.3523C + 0.677509C^2 - 0.0159732C^3 + 0.000144876C^4} \text{ Month}^{-1} \tag{4.1}$$

where C represents temperature in °C. Substituting the temperatures in Table 3 into (4.1), the biting rate of mosquitoes can be approximated by

$$\begin{aligned}\beta(t) &= 7.989 + 0.4487\cos(\pi t/6) + 0.7684\sin(\pi t/6) - 0.4603\cos(2\pi t/6)\\ &\quad - 0.2658\sin(2\pi t/6) - 0.09456\cos(3\pi t/6) - 0.03793\sin(3\pi t/6)\\ &\quad + 0.01472\cos(4\pi t/6) + 0.02339\sin(4\pi t/6) + 0.004283\cos(5\pi t/6)\\ &\quad + 0.05418\sin(5\pi t/6) \quad \text{Month}^{-1}.\end{aligned}$$

Similarly, the temperature-dependent death rate of adult mosquitoes is given by [14],

$$\mu_v(C) = 30.4 + 29.564e^{(-\frac{C-278^\circ K}{2.7035})} \quad \text{Month}^{-1}. \tag{4.2}$$

Then the death rate of adult mosquitoes can be fitted as

$$\begin{aligned}\mu_v(t) &= 3.058 - 0.004607\cos(\pi t/6) - 0.005952\sin(\pi t/6) + 0.003278\cos(2\pi t/6)\\ &\quad + 0.003186\sin(2\pi t/6) + 0.0008082\cos(3\pi t/6) - 0.0008577\sin(3\pi t/6)\\ &\quad - 0.0001089\cos(4\pi t/6) - 000007509\sin(4\pi t/6) + 0.0001428\cos(5\pi t/6)\\ &\quad - 0.0003749\sin(5\pi t/6) \quad \text{Month}^{-1}.\end{aligned}$$

To estimate the maturation function of the mosquito, we suppose that the egg deposition rate is a linear function of the biting rate [14],

$$\Lambda_v(t) = 5 \times \beta(t) \times N_h \quad \text{Mosquitoes} \times \text{Month}^{-1}.$$

In 2018, [25] studied safety and mosquitocidal efficacy of high-dose ivermectin in Kenya adults. They found ivermectin 300 $\mu g/kg$ per day for 3 days provided a good balance between efficacy and tolerability, and reduced mosquito survival for at least 28 days after treatment. It can be seen that this drug shows promise as a potential new tool for malaria elimination. By fitting the data of mosquito survival post treatment in [25], we obtain the ivermectin-induced mortality of mosquitoes on post-treatment days $0, 2+4h, 7, 10, 14, 21$ and 28, see Table 4.

TABLE 4. Ivermectin-induced mortality of mosquitoes.

Ivermectin test times (Day)	**2+4h**	**7**	**10**	**14**	**21**	**28**
Drug-induced mortality	0.7817	0.6782	0.4364	0.3156	0.1479	0.1105

And we can get the following fitted function for the mortality rate of mosquito (see Figure 2)

$$d_v(t) = 0.9668e^{-0.07611t}.$$

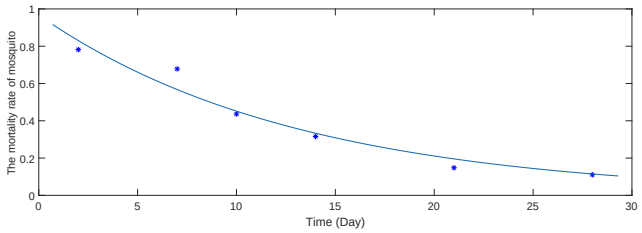

FIGURE 2. Ivermectin-induced mortality of mosquitoes.

4.2. **Model validation.** From [17], We can get data on the monthly malaria cases generated in Kenya from January 2013 to December 2020. From Figure 3, the monthly reported numbers of malaria has pronounced seasonality in Kenya. Based on the estimated parameter values above and the initial values: $S_h(0) = 34850000$, $E_h(0) = 13960$, $I_h(0) = 359300$, $T_h(0) = 517200$, $R_h(0) = 12889000$, $S_v(0) = 247100000$, $I_v(0) = 1236000$, we fit the Kenyan malaria cases by model (2.2). The reported data, the third-order Fourier fitted function for these data and the simulation result in Kenya from January 2013 to December 2015 are shown in Figure 3.

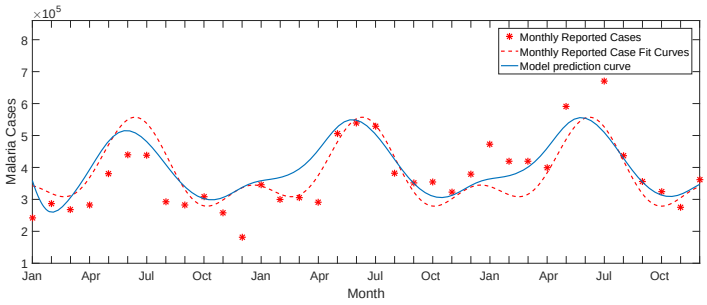

FIGURE 3. Comparison between the reported malaria cases from 2013 to 2015 and the simulation cases form model (2.2).

The numbers of malaria in the future several years in Kenya is shown in Figure 4 with no further effective control measure is taken and the initial values:

$$\begin{gathered} S_h(0) = 37930000, E_h(0) = 53770, I_h(0) = 415200, T_h(0) = 817200, \\ R_h(0) = 8820000, S_v(0) = 246300000, I_v(0) = 1597000. \end{gathered} \tag{4.3}$$

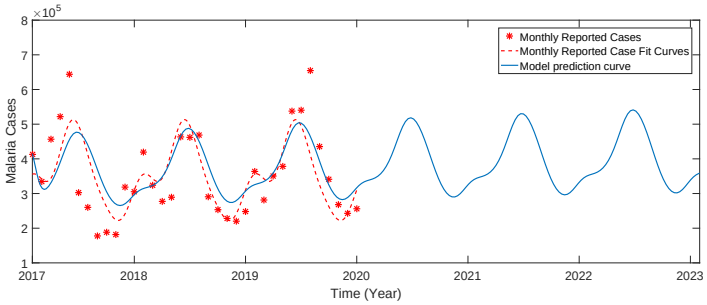

FIGURE 4. Malaria development trend by forecasting model (2.2).

4.3. **Long-term behavior.** In this subsection, we verify of the theoretical results by computing the basic reproduction R_0 and simulating the long-term behavior of the model (2.2) under the same set of parameter values as Figure 3 and initial values (4.3) Assuming that vaccination rate $\kappa = 0.2$, we can obtain $R_0 = 1.0691 > 1$, and the images of I_h and I_v are shown in Figure 5. In this case, the disease persists and eventually shows stable periodical fluctuations. If vaccination rate is increased to $\kappa = 0.7$, then $R_0 = 0.7487 < 1$. In this case, the long-term behavior of infectious

mosquitoes and humans are shown in Figure 6, which implies that malaria will eventually die out. These simulations are consistent with the results of Theorem 3.5 and Theorem 3.6.

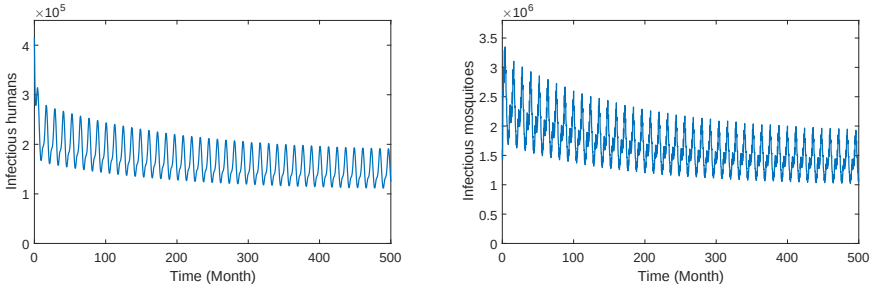

(a) (b)

FIGURE 5. Long-term behaviors of the infectious compartments in model (2.2) when $R_0 = 1.0691$.

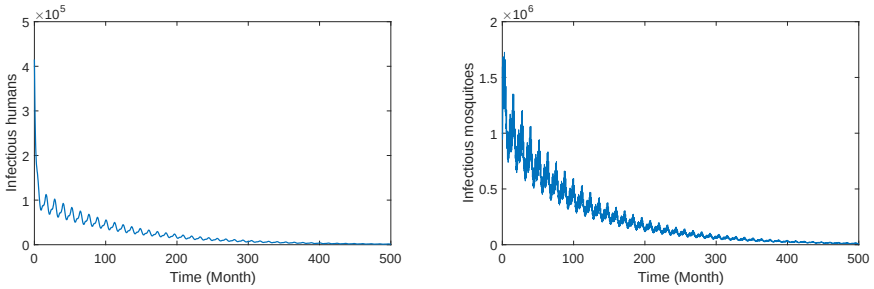

(a) (b)

FIGURE 6. Long-term behaviors of the infectious compartments in model (2.2) when $R_0 = 0.7487$.

4.4. **Sensitivity analysis of R_0.** To explore the effectiveness of ivermectin vaccine in the control of malaria, it is important to analyze the relationship between some parameters of model (2.2) and R_0. We mainly consider the effect of ivermectin vaccination rate κ and mosquito bite rate $\beta(t)$ on R_0. We use the parameter values in Table 2 and the initial values (4.3).

Firstly, we discuss the effect of ivermectin vaccination rate κ on R_0. By keeping the other parameter values the same as those in Table 2, we observe that R_0 is a decreasing function of κ and $R_0 < 1$ when $\kappa > 0.2837$ (see Figure 7a). Therefore, increasing the ivermectin vaccination rate can be an effective way to control malaria transmission.

Then, to simulate the effect of the bite rate $\beta(t)$ on R_0, we make $\kappa = 0$ and replace $\beta(t)$ with $\hat{\beta}(t) = (1-q)\beta(t)$, where q can be considered as the efficiency of people's reduced mosquito bites. Under other parameter values the same as those in Table 2, we observe that R_0 is a decreasing function of q and $R_0 < 1$ when $q > 0.1570$ (see Figure 7b). That means malaria transmission gradually decreases

and will eventually disappear completely by controlling the rate of mosquito bites. Figure 8 gives the graph of R_0 as a function of the parameters κ and q. It can be seen that increasing the values of κ and q is helpful for reducing R_0.

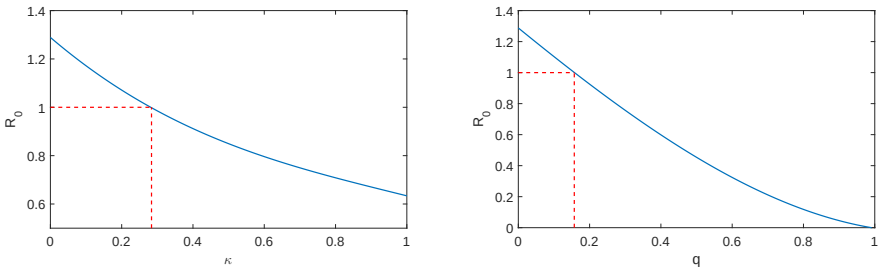

(a) (b)

FIGURE 7. Sensitivity analysis of R_0. **a** Relationship between R_0 and κ. **b** Relationship between R_0 and q.

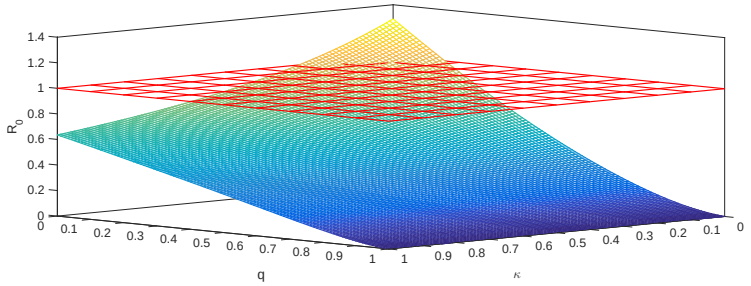

FIGURE 8. Influence of κ and q on R_0.

4.5. **Analysis of the effect of ivermectin.** In this section, we explore the effect of ivermectin on malaria transmission in various regimens of use by model (2.2). We mainly discuss the effect of ivermectin vaccination rate, number of and timing between vaccine intervention rounds on malaria transmission control.

Figure 9 shows the effect of different ivermectin vaccination rate κ on I_h and I_v by 1 month apart of vaccine intervention. We find that the higher value of κ is, the lower level I_h and I_v can be reduced to, and when $\kappa = 1$, malaria disappears after only about 300 months.

Since malaria transmission is seasonal in some areas, adjusting the frequency of administration in line with the malaria transmission season could have an effect on malaria transmission [24]. In addition, seasonal vaccine intervention is easier to administer and also effect in reducing malaria outbreaks. We consider four ivermectin regimens: 3 rounds given 1 month apart, 3 rounds given 2 month apart, 3 rounds given 3 month apart and 4 rounds given 1 month apart (three consecutive daily doses of 300 $\mu g/kg$ per day) and ivermectin vaccination rate $\kappa = 0.7$. As shown in Figure 10, ivermectin has a significant effect on malaria transmission season, the effect of continuous vaccines interventions is greater than that of intermittent

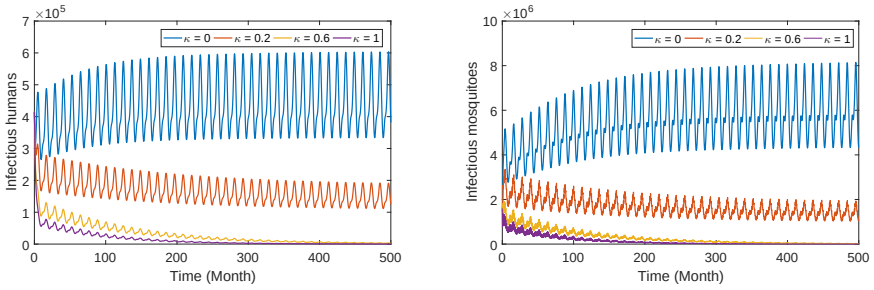

FIGURE 9. Different κ correspond to different infection humans.

vaccines interventions and increases in the vaccines interventions frequency could reduce malaria transmission season. As Kenya is a seasonal malaria transmission country, Figure 10 also shows that the interventions will still have an impact in year 2 and the impact trend is similar to Figure 3.8 in the Appendix of [24] (with different doses of the drug).

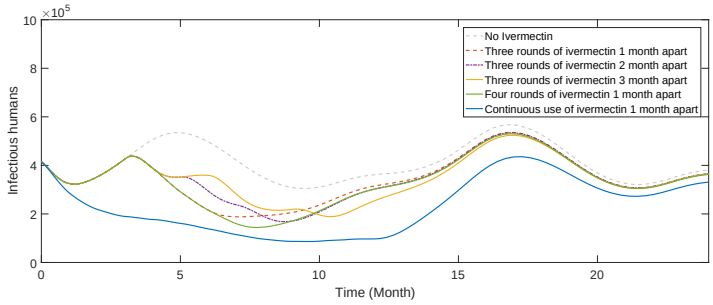

FIGURE 10. Impact of different ivermectin regimens on malaria control.

Using the four ivermectin regimens above, we simulate the long-term behaviors of the infectious humans in Figure 11. We observe that the higher frequency of vaccines interventions is, the lower level $I_h(t)$ can be reduced to.

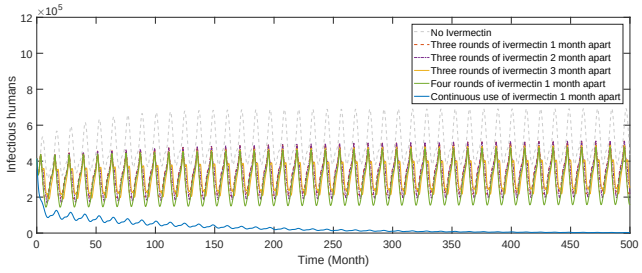

FIGURE 11. Long-term impact of different ivermectin regimens on malaria control.

5. Discussion

Ivermectin is the only drug in the avermectin class of endectocides that is available for human use. It can reduce lifespan of mosquitoes, and also causes secondary behavioural and reproductive disturbances that could affect mosquito survival. Based on the experiment results obtained [6, 7, 25], we developed a delay malaria transmission model incorporating seasonality and ivermectin. The basic reproduction ratio R_0 is derived by the theory developed in [34]. By appealing to the theory of persistence of dynamical systems and the theory of chain transitive sets, we obtained R_0 is the threshold parameter for the extinction and persistence of malaria. That is, if $R_0 < 1$, then infective compartments approach zero eventually; if $R_0 > 1$, then malaria will persist. Numerically, we have estimated all constant and periodic parameters from some published data and studied malaria transmission in Kenya. We verified our theoretical results by simulating the long-term behavior of the solution. By showing a graph of how R_0 varies with ivermectin vaccination rate and bite rate, we found that it is possible to eliminate malaria from Kenya when we combined ivermectin with tools to control bite rates. Furthermore, it takes at least 25 years to eliminate malaria from Kenya with malaria control measures intact (see Figure 9). We also simulated four ivermectin regimens and found that the higher the dosing frequency is, the lower level $I_h(t)$ can be decreased to. Furthermore, our simulation of the effect in year 2 is similar to [24]. Thus, the model is more realistic for the control of malaria transmission.

From the above analysis, we found that ivermectin may be effective in a malaria transmission seasonal. At present, there are many ivermectin-related clinical trials being conducted, for example: one in Guinea-Bissau, one in Thailand and a multisite study in Mozambique and Tanzania [24]. We expected to study the effect of ivermectin by constructing a reasonable mathematical model with these relevant clinical and entomological data, and combining with different transmission settings, different malaria vectors, and different control measures in the future.

Acknowledgments. This research was supported by grants FRF-TP-20-068A1 from the Fundamental Research Funds for the Central Universities.

We are grateful to the anonymous referees for their valuable comments.

References

[1] G. J. Abiodun, et al.; Modelling the influence of temperature and rainfall on the population dynamics of Anopheles arabiensis, *Malar J.*, **15** (2016), 364–379.

[2] F. B. Agusto, N. Marcus, K. O. Okosun; Application of optimal control to the epidemiology of malaria, *Electron. J. Differ. Eq.*, **81** (2012), 1–22.

[3] I. Al-Darabsah, Y. Yuan; A periodic disease transmission model with asymptomatic carriage and latency periods, *J. Math. Biol.,* **77** (2018), 343–376.

[4] S. Bhatt, D. Weiss, E. Cameron, et al.; The effect of malaria control on Plasmodium falciparum in Africa between 2000 and 2015, *Nature*, **526** (2015), 207–211.

[5] C. Boëte, F. B. Agusto, R. G. Reeves; Impact of mating behaviour on the success of malaria control through a single inundative release of transgenic mosquitoes, *J. Theoret. Biol.*, **347** (2014), 33–43.

[6] C. J. Chaccour, et al.; Ivermectin to reduce malaria transmission: a research agenda for a promising new tool for elimination, *Malar J.,* **12** (2013), 153–161.

[7] C. J. Chaccour, et al.; Establishment of the Ivermectin Research for Malaria Elimination Network: updating the research agenda, *Malar J.,* **14** (2015), 243–251.

[8] N. Chitnis, J. M. Hyman, J. M. Cushing; Determining important parameters in the spread of malaria through the sensitivity analysis of a mathematical model, *Bull. Math. Biol.,* **70** (2008), 1272–1296.

[9] B. Dembele, A. -A. Yakubu; Optimal treated mosquito bed nets and insecticides for eradication of malaria in Missira, *Discrete Contin. Dyn. Syst. Ser. B,* **17** (2017), 1831–1840.

[10] D. A. Ewing, C. A. Cobbold, B. V. Purse, M. A. Nunn, S. M. White; Modelling the effect of temperature on the seasonal population dynamics of temperate mosquitoes, *J. Theoret. Biol.*, **400** (2016), 65–79.

[11] J. K. Hale, S. M. Verduyn Lunel; Introduction to functional-differential equations, *Appl. Math. Sci.,* **99**, 1993.

[12] F. Li, J. Liu, X. Q. Zhao; A West Nile virus model with vertical transmission and periodic time delays, *J. Nonlinear Sci.,* **30** (2020), 449–486.

[13] Y. Lou, X. -Q. Zhao; A theoretical approach to understanding population dynamics with seasonal devel opmental durations, *J. Nonlinear Sci.,* **27** (2017), 573–603.

[14] Y. Lou, X. -Q. Zhao; A climate-based malaria transmission model with structured vector population, *SIAM J. Appl. Math.,* **6** (2010), 2023–2044.

[15] G. Macdonald; The epidemiology and control of malaria, *Oxford University Press*, London, UK, 1957.

[16] Mectizan Donation Program. Annual highlights 2020.

[17] Ministry Of Health Data Analytics Platform (MOH DAP).

[18] G.A. Ngwa, et al.; On a three-stage structured model for the dynamics of malaria transmission with human treatment, adult vector demographics and one aquatic stage, *J. Theoret. Biol.,* **481** (2019), 202–222.

[19] K. Okuneye, A. B. Gumel; Analysis of a temperature- and rainfall-dependent model for malaria transmission dynamics, *Math. Biosci.,* **287** (2017), 72–92.

[20] R. N. Price, L. Von Seidlein, N. Valecha, F. Nosten, J. K. Baird, N. J. White; Global extent of chloroquine-resistant Plasmodium vivax: a systematic review and meta-analysis, *Lancet Infect. Dis.,* **14** (2014), 982–991.

[21] R. Ross; The Prevention of Malaria, *John Murray, London*, 1911.

[22] S. G. Ruan, D. M. Xiao, J. C. Beier; On the delayed Ross-Macdonald model for malaria transmission. *Bull. Math. Biol.,* **70** (2008), 1098–1114.

[23] I. Saran, E. M. Maffioli, D. Menya, et al.; Household beliefs about malaria testing and treatment in Western Kenya: the role of health worker adherence to malaria test results, *Malar J.,* **16** (2017), 349.

[24] H. C. Slater, B. D. Foy, K. Kobylinski, et al.; Ivermectin as a novel complementary malaria control tool to reduce incidence and prevalence: a modelling study, *Lancet Infect. Dis.,* **20** (2020), 498–508.

[25] M. R. Smit, E. O. Ochomo, G. Aljayyoussi, et al.; Safety and mosquitocidal efficacy of high-dose ivermectin when co-administered with dihydroartemisinin-piperaquine in Kenyan adults with uncomplicated malaria (IVERMAL): a randomised, double-blind, placebo-controlled trial, *Lancet Infect. Dis.,* **18** (2018), 615–639.

[26] H. L. Smith; Monotone Dynamical Systems: An Introduction to the Theory of Competitive and Cooperative Systems, *American Mathematical Society, Providence, RI*, 1995.

[27] P. O. Sumba, S. L. Wong, H. K. Kanzaria, et al.; Malaria treatment-seeking behaviour and recovery from malaria in a highland area of Kenya, *Malar. J.*, **7** (2008), 245.

[28] The World Bank, Kenya,

[29] The World Bank, Climate Change Knowledge Portal, https://climateknowledgeportal.worldbank.org/country/Kenya/climate-data-historical

[30] B. Tsanou, J. C. Kamgang, J. M. S. Lubuma, et al.; Modeling pyrethroids repellency and its role on the bifurcation for a bed net malaria model, *Chaos Soliton Fractals,* **136** (2020), 109809.

[31] H. Wang, G. Tian; Propagating interface in reaction-diffusion equations with distributed delay, *Electron. J. Differential Equations,* **2021** (2021), no. 54, 1-22.

[32] W. A. Woldegerima, R. Ouifki, J. Banasiak; Mathematical analysis of the impact of transmission-blocking drugs on the population dynamics of malaria, *Appl. Math. Comput.,* **400** (2021), 126005.

[33] World Health Organisation (WHO). https://www.who.int/health-topics/malaria#tab=tab_1

[34] X. Q. Zhao; Basic reproduction ratios for periodic compartmental models with time delay. *J. Dynam. Differential Equations* , **29** (2015), 67–82.
[35] X. Q. Zhao; Dynamical Systems in Population Biology, Second edition, *CMS Books in Mathematics, Springer, Cham*, 2017.

Zhihong Zhao
School of Mathematics and Physics, University of Science and Technology Beijing, Beijing 100083, China
Email address: zzh@ustb.edu.cn

Shaochun Li
School of Mathematics and Physics, University of Science and Technology Beijing, Beijing 100083, China
Email address: leeschun@foxmail.com

Yulan Lu
School of Mathematics and Physics, University of Science and Technology Beijing, Beijing 100083, PR China
Email address: luyulan@ustb.edu.cn